Cotranslational Targeting and Posttranslational Translocation can Cooperate in Spc3 Topogenesis

Sung-jun Jung [1], Ji Eun Hani Kim [1], Tina Junne [2], Martin Spiess [2] and Hyun Kim [1]*

*1 - **School of Biological Sciences and Institute of Microbiology,** Seoul National University, Seoul 08826, South Korea*
*2 - **Biozentrum,** University of Basel, Basel, Switzerland*

Correspondence to Hyun Kim: School of Biological Sciences, Building 504-421, Seoul National University, Seoul 08826, South Korea. *joy@snu.ac.kr (H. Kim)*
https://doi.org/10.1016/j.jmb.2021.167109
Edited by William Clemons

Abstract

Secretory and membrane proteins follow either the signal recognition particle (SRP)-dependent cotranslational translocation pathway or the SRP-independent Sec62/Sec63-dependent posttranslational pathway for their translocation across the endoplasmic reticulum (ER). However, increasing evidence suggests that most proteins are cotranslationally targeted to the ER, suggesting mixed mechanisms. It remains unclear how these two pathways cooperate. Previous studies have shown that Spc3, a signal-anchored protein, requires SRP and Sec62 for its biogenesis. This study investigated the targeting and topogenesis of Spc3 and the step at which SRP and Sec62 act using *in vivo* and *in vitro* translocation assays and co-immunoprecipitation. Our data suggest that Spc3 reaches its final topology in two steps: it enters the ER lumen head-first and then inverts its orientation. The first step is partially dependent on SRP, although independent of the Sec62/Sec63 complex. The second step is mediated by the Sec62/Sec63 complex. These data suggest that SRP and Sec62 act on a distinct step in the topogenesis of Spc3.

Introduction

Most proteins directed for the secretory pathway in eukaryotes are first targeted to the Sec61 translocon in the endoplasmic reticulum (ER). A conventional view of the targeting process is that the N-terminal signal sequence or the first transmembrane (TM) segment of a nascent chain is recognized by the signal recognition particle (SRP), and the ribosome-associated nascent chain complex is escorted to the ER membrane containing the SRP receptor.[1–3] Signal sequences of precursors not recognized by SRP are assumed to be fully synthesized and posttranslationally targeted to the Sec61 complex by cytoplasmic chaperones.[4,5] Targeting and translocation are considered coupled processes, and SRP-dependent and SRP-independent targeting indicate cotranslational and posttranslational translocation, respectively.

However, recent ribosome profiling studies suggest that the protein targeting to the ER are more dynamic than previously assumed.[6–8] These studies showed that ribosomes are targeted to the ER before the signal sequence is emerged. Another study showed that the yeast cytoplasmic chaperone Ssb1, which has been implicated in escorting nascent chains by an SRP-independent, posttranslational targeting pathway, is associated with translating ribosomes and mediates the cotranslational targeting of approximately 30% of ER-destined proteins.[9] Ssb1 and SRP are found to bind precursors that follow the cotranslational targeting route.[9] Therefore, accumulating evidence suggests that most proteins reach the ER cotranslationally.

The Sec61 complex, the main protein-conducting channel, acts as a ribosome receptor in the ER to mediate cotranslational translocation. As membrane proteins emerge from the ribosome, their different parts should be correctly localized to the lumen, membrane, or cytoplasm to generate the correct membrane topology. Single-pass membrane proteins can assume two different membrane topologies: type I (N_{out}-C_{in}) orientation if the N-terminus faces the ER lumen (out) or type II (N_{in}-C_{out}) if the N-terminus faces the cytoplasm (in).[10] The latter group is also called signal-anchored (SA) proteins, as its signal sequence acts in targeting and membrane anchoring in the membrane topology of the cleavable signal sequence.

Two models have been proposed for the topogenesis of SA proteins.[10,11] First, an SA domain enters the ER membrane in a looped conformation.[11,12] Second, an SA domain enters head-on and subsequently inverts to assume a N_{in}-C_{out} membrane topology.[13,14] A previous study on the topogenesis of SA proteins using a set of model proteins showed that the N-terminal region preceding the hydrophobic core of the SA sequence, particularly its length, is critical for whether the nascent chain engages the translocon head-on or in a looped conformation.[15]

The orientation of a TM helix is determined primarily by the distribution of charged amino acids flanking a TM segment, and the soluble side containing positively charged residues tends to face the cytosol (the so-called positive inside rule).[16] However, the TM segment of eukaryotic membrane proteins targeted to the ER often does not contain clear differences in charge distribution between the N- and C-terminal flanking regions. It is unclear how membrane proteins with weak or mixed topogenic signals assume their correct membrane topology and which translocon components mediate topogenesis.

The Sec61 complex interacts with the Sec62/Sec63 complex to form a larger SEC complex in yeast and humans and mediates posttranslational translocation.[17,18] The SEC complex is also involved in the topogenesis of membrane proteins carrying a moderately hydrophobic TM segment.[19,20] A proximity-specific ribosome profiling study has shown that ER-targeted ribosomes associate with nascent chains with SRP-independent signal sequences that follow posttranslational translocation.[7] Furthermore, Ssb1, a cytosolic chaperone associated with the ribosome and the ribosome-bound nascent chain, interacts with Sec72 via its tetracopeptide repeat domain, suggesting the possibility of cotranslational translocation through the SEC complex.[21] However, recent cryo-EM structures of the SEC complex showed that the ribosome and the Sec62/63 complex cannot bind to the Sec61 channel simultaneously because of an overlapping binding site on the cytoplasmic side of the Sec61 complex.[22,23] Hence, it remains unclear how the cotranslationally targeted nascent chain can be posttranslationally translocated via the SEC complex.

Previous studies have shown that Spc3, a SA protein, is an SRP-dependent substrate that is cotranslationally targeted.[4,6,7] Spc3 contains a moderately hydrophobic TM domain with a weak topogenic signal. We previously observed that the biogenesis of Spc3 was impaired in an SRP-defective strain and Sec62 mutant strains.[20,24] This study investigated the topogenesis of Spc3 using glycosylation-based membrane insertion, *in vitro* post-translational translocation assays, and co-immunoprecipitation (co-IP) experiments. Our data suggest that the targeting and initial N-terminal insertion of Spc3 are mediated by SRP; however, it occurs independently of Sec62/Sec63. Subsequent recognition of the head-on inserted Spc3 SA domain, and its inversion requires the Sec62/Sec63 complex. These results suggest that cotranslational targeting and posttranslational translocation can cooperate in the topogenesis of Spc3.

Results

Spc3 enters as a head-on conformation in the ER membrane

Spc3 is a small signal-anchored (SA) protein subunit of the ER signal peptidase complex. It has a cryptic N-linked glycosylation site (N-site) at the N-terminus and two sites in the C-terminal region (Figure 1(A)).[25] Upon natural topogenesis, the two C-terminal N-sites are glycosylated in the ER lumen.

First, we investigated the mode of initial engagement of Spc3 when it entered the ER. The two modes of initial engagement for SA proteins, head-on *versus* loop insertion, differ in that the N-terminus of the former is exposed to the ER lumen during the initial insertion, whereas the latter remains on the cytoplasmic side. To probe the location of the N-terminus of Spc3 during its initial engagement, we engineered an additional N-site at the N-terminal end. N-linked glycosylation exclusively occurs when the consensus N-site sequence N-X-T/S (X, any amino acid except proline) in a protein is exposed to the lumen. In membrane proteins, the N-site should be present at least 15 residues away from the end of the transmembrane (TM) domain.[26] An endogenous N-site is present at the N-terminal flanking region of the TM domain; however, it is too close to be used; therefore, we introduced an additional N-site (NST) 15, 17, and 19 residues away from the end of the SA domain at the N-terminus (Spc3(N), (N2) and (N4)) (Figure 1(A)). In case the addition of three N-site residues at the N-terminus affects topology or topogenesis, we also prepared variants carrying a non-glycosylatable Gln(Q) residue instead of Asn (N) as controls (Spc3(Q)/(Q2)/(Q4)) (Figure 1(A)).

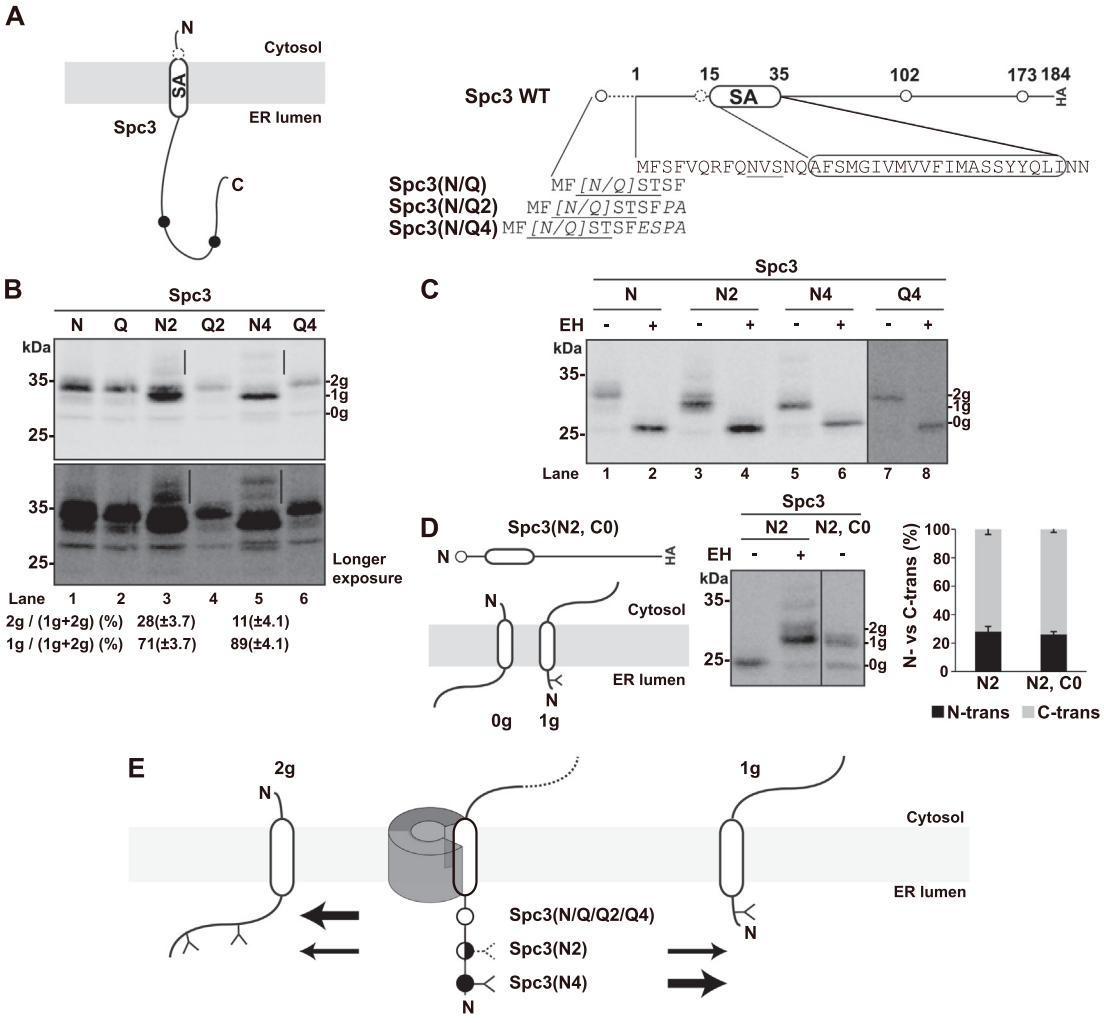

Figure 1. The signal-anchored (SA) domain of Spc3 enters as a head-on conformation. (A) Left: Membrane topology of Spc3. SA indicates a signal-anchored domain. Unfilled and filled circles indicate unused and used N-linked glycosylation sites (N-site). Right: Sequences of the N-terminal region of Spc3 and N-terminal variants are shown. Circles indicate N-sites. A dashed circle indicates a cryptic N-site. The N-site sequences are underlined. Introduced N-terminal amino acids are indicated in italic. (B) Spc3 N-terminal variants in the W303-1α strain were metabolically labeled with [^{35}S]Met for 5 min at 30 °C. The N-linked glycosylation status is indicated on the right side of the autoradiogram (0–2 g). A longer exposed autoradiogram is shown below. Multiply glycosylated bands are indicated with black lines. The relative amounts of 1 g and 2 g were calculated as ([1 g or 2 g × 100/(1 g + 2 g)]). Three independent experiments were carried out and the average and standard deviations are shown. C. Samples from B were incubated with endoglycosidase H (EH) before SDS-gel electrophoresis. (D) Schematics of Spc3(N2) variant lacking the C-terminal two N-sites, Spc3(N2, C0). Spc3(N2) and Spc3(N2, C0) were analyzed by metabolic labeling as done in (B) and (C). The N-linked glycosylation status is indicated on the right side of the autoradiogram (0–2 g). The relative amounts of N-translocated forms ([(1 g × 100)/(1 g + 2 g)] for Spc3(N2), [(1 g × 100)/(0 g + 1 g)] for Spc3 (N2, C0), N-trans), and C-translocated forms ([(2 g × 100)/(1 g + 2 g)] for Spc3(N2), [(0 g × 100)/(0 g + 1 g)] for Spc3 (N2, C0), C-trans) are plotted. At least three independent experiments were carried out and the average and standard deviations are shown. (E) Schematic models for the SA domain insertion of Spc3 variants.

For the head-on insertion, the N-terminal N-site in the Spc3(N) variant would be glycosylated, generating a singly glycosylated form. In contrast, for the loop insertion, the N-terminal N-site would not be glycosylated. To capture the early stage of topogenesis, Spc3 variants were radiolabeled with [^{35}S]Met in yeast cells for 5 min, immunoprecipitated, separated on SDS-gels, and visualized via phosphorimaging. The size of Spc3(N) and Spc3(Q) was shifted down on an SDS-gel upon treatment with endoglycosidase H (Endo H), which removes N-glycans (Figure 1(B), (C), lanes 1 and 2). If the N-terminal N-site was used, the size of Spc3(N) and Spc3(Q) would have been different since Spc3(Q) cannot be glycosylated;

thus, these data indicate that their C-terminal N-sites are glycosylated.

For Spc3(N2), an additional faster-migrating band that was not detected in Spc3(Q2) was observed (Figure 1(B), lanes 3 and 4, Figure 1(C), lane 3). For Spc3(N4), this faster-migrating band was the major product; however, it was not detected in Spc3(Q4), indicating that it resulted from N-terminal glycosylation (Figure 1(B), lanes 5, 6, and Figure 1(C), lanes 5 and 7). These data suggest that the N-terminus initially enters the ER lumen. For Spc3(N) and Spc3(Q), the N-terminus entered the lumen; however, the N-site was too close to the membrane for oligosaccharyltransferase (OST) to recognize, and the SA domain reoriented to form a type II membrane topology (2 g) (Figure 1(E), left). For Spc3(N2), which has two more residues than Spc3(N), the N-terminal N-site is now at the threshold length from the membrane for OST access. The N-terminal N-site becomes glycosylated for some, whereas others are quickly inverted and the C-terminal N-sites become glycosylated, resulting in N-translocation and C-translocation forms, respectively (Figure 1(E)). To confirm that the singly glycosylated form is a result of glycosylation of the N-terminus, but not due to inefficient glycosylation of the C-terminus, we prepared an Spc3(N2) variant lacking the C-terminal N-sites (Spc3(N2, C0) (Figure 1(D)). If a singly glycosylated form in Spc3(N2) results from inefficient glycosylation of the C-terminal N-sites, a singly glycosylated form would not appear for the Spc3(N2, C0) variant. However, a singly glycosylated form was observed for Spc3(N2, C0), indicating N-terminal translocation. For this variant, a singly glycosylated form indicates N-translocation, whereas an unglycosylated form indicates C-translocation or an untranslocated form. Given that all Spc3 variants are efficiently targeted, it is unlikely that the unglycosylated species of Spc3(N2, C0) represent the untranslocated form. When the relative amounts of N- and C-translocated forms of Spc3(N2) and Spc3 (N2, C0) were compared, similar levels were observed (Figure 1(D)). These data thus confirm that the singly glycosylated form of Spc3(N2) results from N-translocation. For Spc3(N4), the N-terminal N-site was further away from the membrane, the N-terminal N-site was efficiently glycosylated, and the addition of polar glycans prevented reorientation, resulting in primarily N-translocation (Figure 1(E), right). The N-terminus of Spc3(Q2) and Spc3(Q4) also entered the lumen, although without glycosylation, it could reorient and form a type II topology (Figure 1(E), left). Although we cannot rule out the possibility that one more methyl group in Q compared to N in Spc3(Q4) variants might cause its insertion as a loop instead of head-on, data from the pattern of glycosylation in all six variants suggest that Spc3 is likely to insert head-on.

The C-terminal translocation follows the head-on insertion

For Spc3(N2) and Spc3(N4), where the N-terminal N-site was modified, we observed that multiple glycosylated forms (3 g and 4 g) appeared (Figure 1(B), lanes 3 and 5, indicated by black lines). To investigate them in detail, we performed pulse-chase experiments in Spc3(Q4), which the N-terminal N-site was not present, only the C-terminally translocated, doubly glycosylated product was detected during the chase (Figure 2(A), lanes 5–8). In comparison, Spc3(N4) mostly generated singly (1 g) glycosylated products at 0 min, representing the N-terminally translocated form; however, multiple glycosylated products with three or even four glycans were detected. Their intensity increased during the chase, whereas the relative amount of the 1 g form decreased when assessed in the presence of the proteasome inhibitor, MG132 (Figure 2(A), graph). These data indicate that C-terminal glycosylation occurred when N-terminal glycosylation occurred.

To confirm the location of the 4-fold glycosylated form in Spc3(N4), we assessed the membrane association of the 4 g form of Spc3(N4) by carbonate extraction (Figure 2(B)). Control proteins, CPY, a soluble protein, and Dap2, an SA protein, were detected in the supernatant and pellet fractions, respectively. The 1 g form of Spc3 (N4) was found in the pellet fraction, whereas the 4 g form was mostly found in the supernatant fraction, confirming that the 1 g form is membrane-anchored, although the 4 g form is not.

Thereafter, we performed a proteinase K (PK) protection assay to confirm the localization of the Spc3(N4) 4 g form and membrane topologies of Spc3 wild-type (WT) and Spc3(N4) (Figure 2(C)). 40[Leu16]CPY was used as a control. 40[Leu16] CPY is a previously characterized model protein consisting of a cytosolic N-terminal domain of 40 residues, an SA domain of 16 leucines, followed by the sequence of carboxypeptidase Y (CPY) with a C-terminal HA tag.[27] Upon addition of PK, the cytosolic N-terminal 40 residues were digested, indicating its N_{in}-C_{out} topology. Spc3 WT was protected from PK digestion, confirming its N_{in}-C_{out} topology. For Spc3(N4), most of the 1 g form was digested, indicating that its C-terminus faces the cytoplasm after completion of translation. In contrast, the 4 g form is protected from PK digestion, indicating that it is in the lumen. These data suggest that the head-on insertion of Spc4(N4) occurs first, followed by posttranslational C-terminal translocation.

Targeting and head-on insertion of Spc3 are independent of Sec62 and Sec63

Previously, we observed that the biogenesis of Spc3 is dependent on both SRP and Sec62.[24] To assess the stage at which SRP and Sec62 function

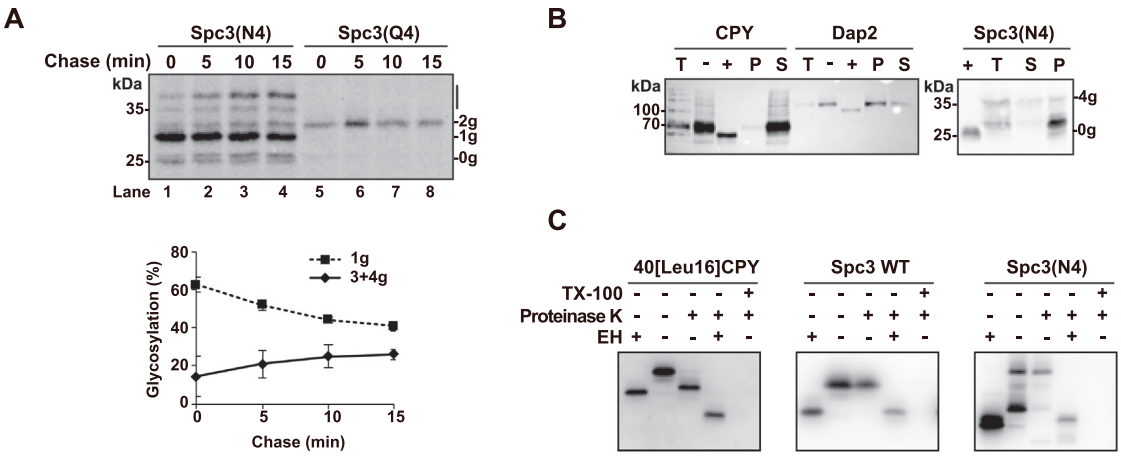

Figure 2. The N-terminal-inserted Spc3(N4) undergoes C-terminal translocation. (A) Spc3(N4) or Spc3(Q4) in the W303-1α strain were metabolically labeled for 5 min and chased for the indicated time in the presence of MG132. Black lines indicate multiply glycosylated bands (3 g and 4 g). The relative amounts of multiply (3 g + 4 g) and singly (1 g) glycosylated products were calculated as [(3 g + 4 g or 1 g species × 100)/Total]. At least three independent experiments were carried out and the average and standard deviations are shown. (B) The indicated proteins were analyzed by a carbonate extraction. Endo H was added to Total (T) fractions (±). Proteins were visualized by Western blotting using HA antibody. P, pellet and S, supernatant fractions. (C) The indicated proteins were analyzed by Proteinase K protection assays. After crude membrane fractionation, Proteinase K was added in the presence or absence of Triton X-100 (TX-100). Endo H was added in the indicated lanes. Proteins were visualized by Western blotting using HA antibodies.

topogenesis of Spc3, we examined the insertion of Spc3 in *sec62* (*sec62_35DDD* and *sec62_219A)* and SRP (*sec65-1*) mutant strains. Mutations in the N-terminus (*sec62_35DDD*) disrupted the binding of Sec62 to Sec63 and impaired the membrane insertion of proteins carrying the marginally hydrophobic TM domain.[19] A single point mutation at the cytosolic interfacial region of TM2 of Sec62 (*sec62_219A*) exhibited a similar phenotype despite retaining its association with Sec63.[19,28] These strains do not cause general translocation and glycosylation defects; however, they selectively impair the translocation of a subset of proteins. The cotranslational translocation substrate Dap2 was translocation-defective in the SRP mutant strain but not in the *sec62* mutant strain. In contrast, the posttranslational translocation substrate CPY was translocation-defective in the *sec62* mutant strain but not in the SRP mutant strain (Figure 3(A)).

Spc3(N4) was expressed, and its N-terminal glycosylation was assessed. Glycosylation levels of Spc3(N4) in WT and *sec62* mutant strains were comparable, whereas the unglycosylated product was increased in the SRP-defective strain, suggesting that targeting and head-on insertion are independent of Sec62 but partially dependent on SRP (Figure 3(B)).

We also assessed the translocation of Spc3(N4) in the *sec63* mutant (*sec63_179T*) strain. A point mutation at residue 179 in the luminal J-domain of Sec63 impairs the interaction with the luminal chaperone Kar2 and causes a translocation defect.[29] The head-on insertion of Spc3(N4) occurred efficiently in the *sec63* mutant, as in the *sec62* mutant strains, indicating that targeting and head-on insertion are independent of the Sec62/Sec63 complex (Figure 3(B)).

Spc3(N4) was overexpressed and modified in the N-terminus. Therefore, we also assessed the targeting of endogenous Spc3 expressed under its own promoter. We inserted the HA sequence into the 3′ end of the *SPC*3 gene in the chromosomes of the WT and *sec65*-1 strains and evaluated its expression by pulse-labeling (Figure 3(C)). Spc3-HA was efficiently glycosylated in the WT or the *sec65*-1 strain at the permissive temperature (24 °C), whereas the unglycosylated product was significantly increased upon shifting to the non-permissive temperature (37 °C). These data suggest that endogenous Spc3 is targeted by SRP *in vivo*.

Thereafter, we performed an *in vitro* posttranslational translocation assay in the presence of yeast microsomes to determine whether the head-on insertion of Spc3 occurs posttranslationally (Figure 3(D)). ppαF, which is posttranslationally translocated in yeast microsomes, was used as a control. To monitor the head-on insertion by glycosylation, we used the Spc3(N4) variant and prepared a fusion construct containing the N-terminal Spc3(N4) SA domain in place of the signal sequence of ppαF (Spc3(N4)-pαF) in case the pαF domain affects *in vitro* posttranslational translocation. As ppαF was glycosylated, indicating translocation into the yeast microsomes, no glycosylated product was

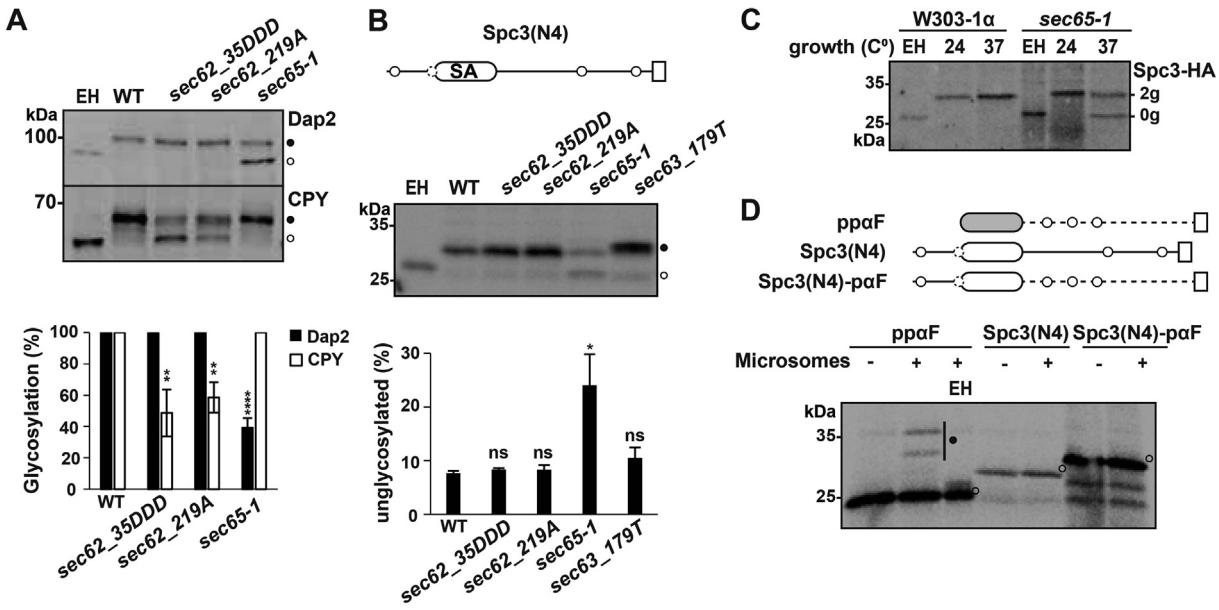

Figure 3. The head-on insertion occurs independent of Sec62 and Sec63. (A and B) Dap2, CPY (A) or Spc3(N4) (B) in wild-type (WT), *sec62_35DDD*, *sec62_219A*, *sec65-1*, and *sec63_179T* (B) strains were radiolabeled with [^{35}S] Met for 5 min and their glycosylation status was assessed. Glycosylation was calculated as [(glycosylated × 100)/ Total] in A. Average values of at least three independent experiments and the standard deviation are shown. Unglycosylated (%) was calculated as [(unglycosylated band × 100)/Total] in B. Average values of at least three independent experiments and standard error are shown. p-values calculated by unpaired *t*-test; *n.s.*, $p > 0.05$; *, $p \leq 0.05$; **, $p \leq 0.01$; ****, $p \leq 0.0001$. (C) Spc3-HA expressed under endogenous promoter in the chromosomes of W303-1α and *sec65-1* strains were radiolabeled for 10 min, 24 °C indicates permissive and 37 °C, nonpermissive temperatures. 2 g and 0 g indicate a properly membrane inserted, doubly glycosylated form and an untargeted form, respectively. (D) The indicated proteins were translated *in vitro* and mixed with yeast microsomes. Filled and open circles indicate translocated and untranslocated products, respectively. EH indicates Endoglycosidase H addition.

detected for Spc3(N4) and Spc3(N4)-pαF. These data suggest that the Spc3(N4) SA domain, in contrast to the signal peptide of ppαF, is not sufficient for posttranslational insertion *in vitro*.

Sec62 and Sec63 mediate inversion of the SA domain of Spc3

To assess the inversion of the Spc3 SA domain, we prepared variants containing only a single N-site at position 175 in the C-terminal domain (Spc3(N175)), and determined their glycosylation in the *sec62* and *sec63* mutant strains (Figure 4 (A) and (B)). Glycosylation of the N-site at 175 was markedly reduced in the *sec62_35DDD* strain, where the interaction between Sec62 and Sec63 was impaired, and in the *sec63_179T* strain, where the interaction between Sec63 and Kar2 was impaired, whereas no defects were observed in the *sec62_219A* strain (Figure 4(B)). These results suggest that the association of Sec62 with Sec63, and the interaction of Sec63 with Kar2 may be critical for the reorientation of the Spc3 SA domain.

To assess the roles of Sec62 and Sec63 in the inversion of the SA domain with unfavorable topogenic signals, we prepared an Spc3 variant with positively charged Lys (K) residues at the C-terminal flanking region of the SA domain (Figure 4(A)). This replacement did not affect the final topology of Spc3. However, it slowed the reorientation of the SA domain due to the positive flanking charges, as shown by the pulse-chase experiments (Figure 4(C)). When the glycosylation of Spc3(KK, N175) was assessed in the *sec62* and *sec63* mutant strains, we found that glycosylation was decreased, even in the *sec62_219A* strain (Figure 4(D)), suggesting that Sec62 function is particularly required to invert an SA domain with poor topogenic information.

Sec62 mediates the inversion of the SA protein that follows the head-on insertion. To determine whether Sec62 specializes in the topogenesis of SA proteins that follow the head-on insertion and inversion mode or whether it also functions on those inserts in a loop conformation, we assessed the topogenesis of previously characterized [Leu16]CPY and 40[Leu16]CPY, N-terminal and internal SA proteins, respectively,[27] in *sec62* defective strains (Figure 4(E)). It has been shown that N-terminal SA proteins such as the [Leu16] variant insert head-on, whereas internal SA proteins such as the 40[Leu16] variant insert in a loop conforma-

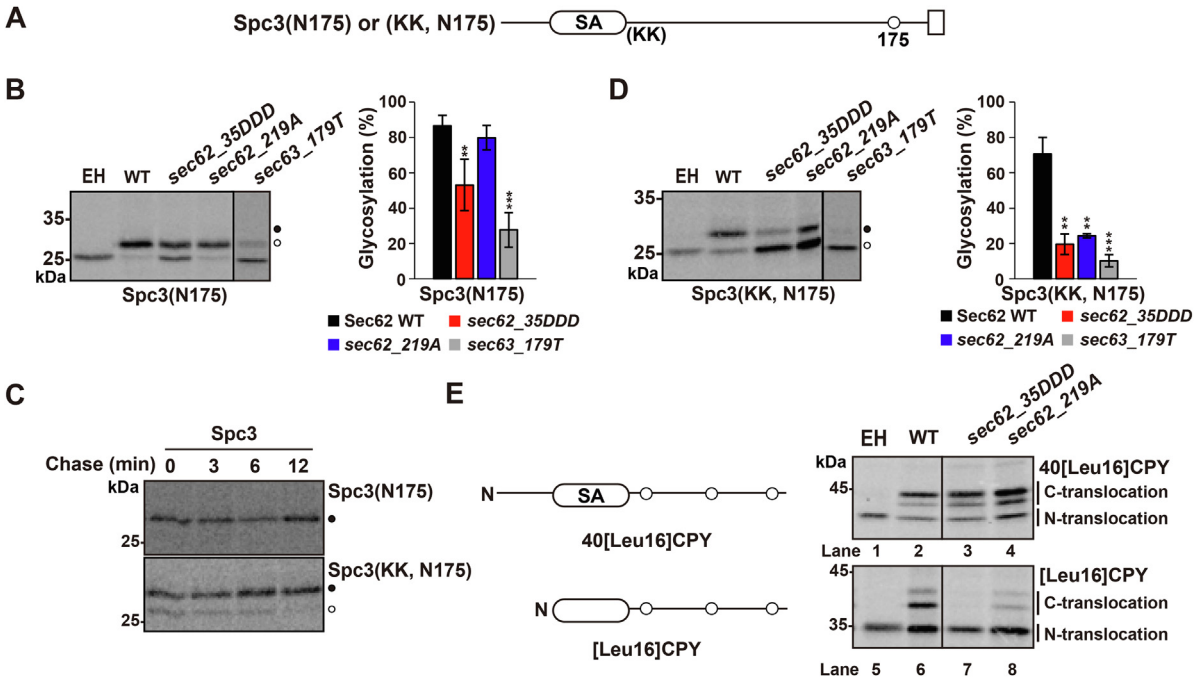

Figure 4. Inversion of SA domain is mediated by Sec62 and Sec63. (A) Schematics and sequences of Spc3(N175) and (KK, N175) with a single N-site at the C-terminus. (B and D) Spc3(N175) and (KK, N175) in the WT, *sec62_35DDD*, *sec62_219A*, and *sec63_179T* strains were subjected to 5 min radiolabeling and analyzed by SDS-PAGE and autoradiography. The average and standard deviation of at least three independent experiments are shown. p-values were calculated by unpaired *t*-test; *n.s.*, $p > 0.05$; **, $p \leq 0.01$; ***, $p \leq 0.001$. (C) Spc3(N175) and Spc3(KK, N175) were metabolically labeled for 3 min and chased for the indicated time in the presence of MG132. Proteins were analyzed by sodium dodecyl sulfate–polyacrylamide gel electrophoresis and autoradiography. The filled and open circles indicate the translocated and untranslocated products, respectively. (E) [Leu16]CPY and 40 [Leu16]CPY in the WT, *sec62_35DDD* and *sec62_219A* strains were radiolabeled for 5 min, and analyzed via SDS-PAGE and autoradiography.

tion.[15] These constructs were initially designed to study the features influencing SA orientation, that is, the flanking charges and the length of the N-domain; hence, both constructs generate a mixture of N- and C-translocations. It was previously confirmed by trypsin digestion and alkaline extraction that the unglycosylated forms are N-translocated and the glycosylated forms are C-translocated in the ER membrane.[27]

The topogenesis of 40[Leu16]CPY in the *sec62* mutant strain was comparable to that in the WT strain (Figure 4(E)). However, C-translocation of [Leu16]CPY was significantly reduced in *sec62* mutant strains, suggesting that Sec62 is important for topogenesis of SA proteins that insert head-on and reorient to assume type II membrane topology.

Sec62 and Sec63 mediate the C-terminal translocation of the head-on inserted Spc3(N4)

To determine whether the C-terminal translocation after the N-terminal insertion of Spc3 (N4) is mediated by Sec62 and Sec63, we performed a pulse-chase experiment with Spc3 (N4) in the WT, *sec62_35DDD*, and *sec63_179T* strains (Figure 5(A)). Although the relative amount of 3 + 4 g forms was increased at 15 min chase in the WT strain, they were markedly reduced at the same time point in the *sec62_35DDD* and *sec63_179T* strains. The multiple glycosylated forms of Spc3(N2) were detected in WT and SRP-defective strains, but not in the *sec62_35DDD* and *sec63_179T9* strains at 5 min pulse-labeling (Figure 5(B)). These results suggest that the N-terminal insertion of Spc3(N4) and Spc3(N2) occurs independently of the Sec62/Sec63 complex, but the subsequent C-terminal translocation occurs by the Sec62/Sec63 complex. Inversion of the signal-anchor and C-terminal translocation may occur simultaneously for reorientation of the head-on inserted intermediate form of an SA protein. For Spc3(N4) and Spc3(N2), inversion of the signal-anchor was prevented due to glycosylation of the head-on inserted form, whereas the C-terminal translocation still must have proceeded by the Sec62/Sec63 complex.

The head-on inserted Spc3(N4) interacts with Sec62

Since the head-on insertion of Spc3(N4) is independent of Sec62, but the follow-up C-terminal translocation is dependent on Sec62, we

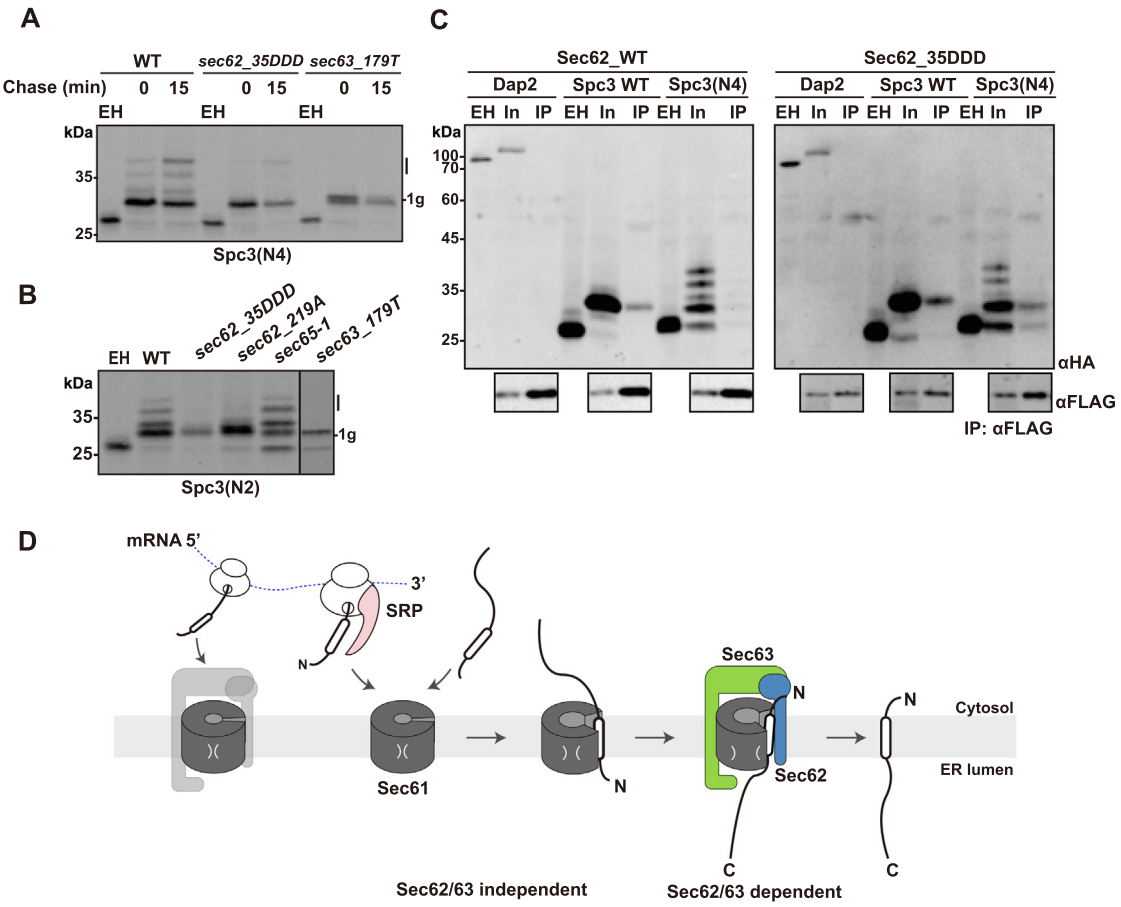

Figure 5. Sec62 interacts with the head-on inserted Spc3(N4). (A) Spc3(N4) in the W303-1α, *sec62_35DDD* and *sec63_179T* strains was metabolically labeled for 5 min and chased for 0 and 15 min. Black lines indicate multiply glycosylated bands (3 g + 4 g). A representative of three experiments is shown. (B) Spc3(N2) was pulse-labeled for 5 min and analyzed by SDS-PAGE and autoradiography. (C) Dap2-HA, Spc3WT-HA and Spc3(N4)-HA in the JRY4 strain carrying a plasmid bearing *SEC62* WT-FLAG or *sec62_35DDD*-FLAG under *SEC62* endogenous promoter were expressed and solubilized with buffer containing 1.2% Triton X-100 and immunoprecipitated with FLAG antibodies at 4 °C overnight. Proteins were analyzed via SDS-PAGE and western blotting with HA or FLAG antibodies. EH: Endo H addition, In: input, IP: immunoprecipitatants B. Proposed model of cotranslational targeting and Sec62/Sec63-mediated posttranslational translocation of Spc3.

assumed that Sec62 may recognize the head-on inserted Spc3(N4) and set out to determine their interaction using co-IP (Figure 5(C)). As a negative control, Dap2, which inserts independently of Sec62, was used.[30] A head-on-inserted, singly glycosylated Spc3(N4) was co-immunoprecipitated with the Sec62_35DDD mutant, whereas multiple glycosylated Spc3(N4) was not, suggesting that Sec62 primarily interacts with the head-on inserted form. Spc3 WT and the Sec62_35DDD mutant were also coimmunoprecipitated. This could be due to a prolonged association between mutant Sec62 and the SA domain of Spc3, even after C-terminal translocation. Compared to the 5 min pulse-labeling, the degree of defect observed for Spc3 WT in the *sec62_35DDD* mutant strain at steady-state level was milder, probably due to faster degradation of untranslocated species. No immunoprecipitation between Spc3(N4) and Sec62 WT was detected, indicating that their association may be too transient to detect. A minor fraction of Spc3 was coimmunoprecipitated with Sec62 WT. As the expression level of Spc3 was high, it was likely a non-specific interaction. A control protein, Dap2, was not immunoprecipitated with Sec62 (Figure 5(C)). Therefore, these data suggest that Sec62 recognizes the head-on-inserted form of Spc3(N4).

Discussion

Translocation of Spc3, an SA protein, occurs via the SRP-dependent cotranslational translocation pathway.[4,6,7] We found that it is also dependent on Sec62, suggesting a posttranslational translocation.[20] Therefore, Spc3 may take cotranslational and postranslational translocation pathways or be cotranslationally targeted via SRP and posttranslationally translocated through the Sec62/Sec63 complex. This study dissected the topogenesis of Spc3

and identified the steps at which SRP and Sec62 act.

Our data suggest a model in which Spc3 is cotranslationally targeted and head-on inserted into the ER membrane, partially dependent on SRP but independent of the Sec62/Sec63 complex (Figure 4(D)). The first round of targeting to the ER is dependent on SRP and occurs cotranslationally *in vivo*, as recent ribosome profiling studies have suggested.[6,7] The 5′ side of the transcript from the first round of targeting would be available for the next round of translation, whereas the 3′ side is still attached to the ribosome-associated with the Sec61 complex. In this case, the transcript is already near the ER translocon; thus, it is possible that the N-terminus of the nascent chain engages the SEC complex independent of SRP. This may explain why targeting of Spc3 is only partially dependent on SRP. Alternatively, initial head-on insertion occurs posttranslationally; however, it is independent of the Sec62/Sec63 complex. The head-on inserted Spc3 SA domain is then recognized by Sec62 in the ER membrane. The hydrophobicity of the TM domain is possible to play a critical role in channel gating. Hydrophobic SA sequences that do not require the Sec62/Sec63 complex are sufficient to open the channel and initiate translocation by themselves. However, moderately hydrophobic and incorrectly positioned signal sequences or TM segments are insufficient to open the Sec61 channel on their own, thus requiring the Sec62/Sec63 complex. The association of the Sec62/Sec63 complex with the Sec61 complex fully opens the channel, as observed in the cryo-EM structures of the SEC complex.[22,23,31] A recent structure of the SEC complex with a bound ppαF shows that the signal sequence was positioned between the lateral gate of the Sec61 and Sec62 TM domains, and the pore was further widened compared to the signal sequence unbound structures.[32] The Sec63_179T mutant, causing an impaired interaction with Kar2,[29] was unable to translocate the C-terminus of Spc3; hence, their interaction may be crucial in the reorientation step of Spc3 topogenesis. An earlier study showed that Sec63 and Kar2 are required for translocation of SRP-dependent substrates.[33]

Our study presents an unchartered example of SA protein topogenesis that involves SRP-dependent targeting with head-on insertion and Sec62/Sec63-dependent inversion of the SA domain. This finding provides mechanistic insights into how cotranslational targeting and posttranslational translocation can cooperate with ER-destined proteins in eukaryotic cells.

Materials and Methods

Yeast strains

W303-1α (*MATα, ade2, can1, his3, leu2, trp1, ura3*) was used as the wild-type strain and a background strain for mutations in this study.[34] The *sec65-1* strain (*MATα, sec65-1, ade2, can1, his3, leu2, trp1, ura3*) is a temperature-sensitive SRP-defective strain.[34] For genomic HA tagging of Spc3 in W303-1α and *sec65-1* strains, a 3xHA-KanM cassette containing complementary sequences to the C-terminal end and 3′ UTR region of Spc3 was inserted by homologous recombination.[35] Sec62 strains contain pRS415 1 kb upstream + *SEC62* (WT) or mutant versions (residues–35-37RQG changed to DDD; 35DDD and P at residue 219 changed to A; 219A) in the JRY4, *sec*62Δ strain (*MATα, sec*62Δ*::HIS3, ade2, can1, his3, leu2, trp1, ura3,* [pRS416 1 kb upstream + *SEC62*]).[19] The pRS416 1 kb upstream + *SEC62* (WT) vector was removed by FOA selection. The Sec63 mutant strain contains pRS415 *sec63_179T* (residue 179A changed to T) in the *sec*63Δ strain (*MATα, sec*63Δ*::HIS3, ade2, can1, his3, leu2, trp1, ura3*).[24] For the co-IP experiment, the JRY4 strain carrying the pRS415 vector with *Sec62 WT_FLAG* or *sec62_35DDD-FLAG* under the endogenous promoter was used.

Construction of plasmids

All plasmids were constructed by homologous recombination of PCR products encoding a protein of interest and *SmaI-linearized* pRS plasmids, as previously described.[20] The PCR products of gene-coding regions were flanked by 30 bases complementing up and downstream of the *SmaI* site sequence in the pRS vector. For *in vitro* translation, PCR products were subcloned into the pGEM vector using a Gibson assembly kit (NEB, USA) following the manufacturer's protocol or DNA ligation. Sequences were confirmed via DNA sequencing.

Model proteins

For 40[Leu16]CPY and [Leu16]CPY, from the constructs in Goder *et al.*[27], EK32/33 (residues 32–33 are E and K) and S47 (P at residue 47 changed to S) versions were used, except for the following cases. For the PK digestion experiment shown in Figure 4(B), 40[Leu16]CPY with the P47 version was used.

Spc3(N175) and Spc3(KK, N175) have two additional residues, PA between F4 and V5 in wild-type Spc3. N104 was mutated to Q in Spc3 (N175) and Spc3(KK, N175). For Spc3(N2, C0), the N residues of the two C-terminal N-sites were changed to Q in Spc3(N2).

Pulse labeling and pulse-chase experiments

Pulse labeling and pulse–chase experiments were performed as previously described[19,20] with the following modifications. Yeast cells expressing model proteins were grown at 30 °C until the OD_{600} reached the log phase. A total of 1.6 OD_{600}

units of cells were used. Beads were washed two times with IP buffer, and once with ConA buffer, and Buffer C, and proteins were resuspended in SDS-PAGE sample buffer (50 mM Tris-HCl, pH 7.5, 5 % SDS, 5 % glycerol, 50 mM EDTA, pH 7.4, 50 mM DTT, 1X protease inhibitor cocktail, 1 mM PMSF) at 95 °C for 5 min. Proteins were subjected to SDS-PAGE and visualized using autoradiography. For pulse labeling with *sec65-1*, 1.6 OD_{600} unit cells were cultured at 24 °C. When the OD_{600} reached the log phase, cells were transferred to 37 °C for 30 min before harvest and starved at 37 °C (nonpermissive temperature) for 15 min. The cells were labeled for 5 min at 30 °C. For pulse labeling assays (Figure 3(C)), cells were cultured at 24 °C. When OD_{600} reached 0.2, cells were further incubated at 24 °C or transferred to 37 °C for 4 h before 5 OD_{600} unit harvest and starved at 24 °C (permissive temperature) or 37 °C (nonpermissive temperature) for 15 min. The cells were labeled for 10 min at 24 °C. For labeling of *sec63_179T* cells, cells were starved at 37 °C for 15 min and labeled at 30 °C for 5 min. For pulse/chase experiments without MG132, 1.6 O.D unit cells per time point were used. Labeling was stopped by adding 50 mM (final concentration) of cold methionine at the 0 min time point. The cells were harvested at the indicated time points. Subsequent procedures were performed as described in the pulse-labeling experiment. For pulse/chase experiments with MG132, cells were cultured in MPD medium containing a nitrogen base without ammonium sulfate and supplemented with the appropriate amino acid drop-out mix and 0.2% proline. When the OD_{600} reached 0.5–1.0, the cells were diluted to 0.5 OD_{600} and grown further at 30 °C in the presence of 0.003% SDS for 3 h. At each time point, 1.6 OD_{600} units of cells per time point were harvested, washed once with MPD-Met media, and resuspended in the same medium containing 0.1 mM MG132. After 30 min of starvation at 30 °C, cells were resuspended in 150 μL MPD-Met medium containing 0.1 mM MG132 per time point and labeled with [^{35}S]Met. Subsequent procedures were performed as in the pulse/chase experiments without MG132.

Carbonate extraction

W303-1α cells expressing each model protein were grown at 30 °C overnight, and 5–10 OD_{600} units of cells were harvested. Cells were resuspended in lysis buffer (20 mM Tris-HCl pH 7.5, 10 mM EDTA, pH 7.4, 100 mM NaCl, 300 mM sorbitol, 1 mM PMSF, and 1X protease inhibitor cocktail) and lysed by bead beating for 10-15 min at 4 °C. After short centrifugation, the supernatant was recovered, and the beads were washed with lysis buffer. The combined supernatants were centrifuged at maximum speed in a desktop centrifuge to remove cell debris. The supernatant (50–100 μl) was stored as 'total'. The remaining samples were mixed with 300 μl of 0.1 M Na_2CO_3 (pH 11.5) and incubated on ice for 30 min. After centrifugation, supernatants were recovered and pellets were washed with 200 μl of 0.1 M Na_2CO_3 (pH 11.5) and combined with the supernatants. Each fraction was incubated with 12.5% TCA on ice for 30 min. Precipitated proteins were pelleted and mixed with SDS-PAGE sample buffer. Proteins were analyzed by sodium dodecyl sulfate–polyacrylamide gel electrophoresis and western blotting using HA antibodies.

Proteinase K protection assay

1.5 OD_{600} units of RSY1293 cells (*MATα, ura3-1, leu2-3,-112, his3-11,15, trp1-1, ade2-1, can1-100, sec61::HIS3*, [pDQ1])[36] expressing each model protein were harvested, resuspended in 150 μl protease digestion buffer (50 mM Tris-HCl, pH 7.5, containing freshly added 30 mM DTT), and lysed with glass beads. After removal of unbroken cells by two consecutive low-speed centrifugations (1000*g*, 10 min), 85 μl of the supernatant was incubated for 45 min on ice with 15 μl of protease digestion buffer with or without Proteinase K (30 μg final) in the presence of 0.5% Triton X-100, where needed. The reaction was stopped with 20% trichloroacetic acid (final concentration). Precipitated proteins were analyzed by SDS-PAGE (12.5%) and western blotting using a rabbit anti-HA antibody (C29F4 from Cell Signaling Technology).

Yeast microsome preparation

From 1 L of yeast culture, cells were harvested when the OD_{600} reached between 1 and 3. Cells were incubated with TSD buffer (100 mM Tris-sulfate, pH 9.4, 10 mM DTT) for 10 min at 25 °C. After centrifugation, spheroplasts were obtained by 20–30 mg of Zymolyase 20 T (US biological, USA) treatment in 50 ml spheroplasting buffer (0.75 × YP, 2% glucose, 1.2 M sorbitol, 20 mM Tris-HCl, pH 7.5) for 30 min at 30 °C. Spheroplasts were washed twice with 1x PBS supplemented with 1.2 M sorbitol. Washed spheroplasts were homogenized twice with 20 strokes of a Dounce homogenizer at 2500 rpm at 4 °C. Unbroken cells, nuclei, and mitochondria were removed by sequential centrifugation. Post-mitochondrial fractions were layered on 30% glycerol cushion (20 mM HEPES-KOH, pH 7.4, 2 mM EDTA, pH 7.4, 200 mM sorbitol, 50 mM KOAc, 1 mM DTT, 1 mM PMSF, and 1x protease inhibitor cocktail. The ER fraction was washed once with washing buffer (50 mM triethanolamine, pH 7.5, 50 mM EDTA, pH 7.5, 1 M NaCl, 250 mM sucrose, 1 mM DTT), and resuspended and stored in storage buffer (50 mM triethanolamine, pH 7.5, 250 mM sucrose, 1 mM DTT). Microsomes were quickly frozen in liquid nitrogen and stored at −80 °C.

In vitro translation and translocation assay

The pGEM vector carrying the gene of interest was added to the TNT *in vitro* transcription and translation coupled kit (Promega, USA). The samples were incubated at 30 °C for 1 h. Isolated yeast microsomes were added to the reaction and incubated for 30 min. Thereafter, 2X SDS-PAGE sample buffer was mixed and boiled at 95 °C for 4 min. The unresolved fraction was removed by centrifugation at 17,000 rpm for 3 min. Proteins were analyzed by sodium dodecyl sulfate–polyacrylamide gel electrophoresis and autoradiography.

Co-IP

Co-IP experiments were performed as described in Zhang *et al.*[37], with the following modifications. Twenty OD_{600} units of JRY4 cells expressing Sec62 WT-FLAG or Sec62_35DDD-FLAG under the endogenous promoter and each model protein were harvested, resuspended in 400 μl 0.1% Triton X-100 buffer (50 mM HEPES-KOH, pH 6.8, 0.1 % TX-100, 150 mM KOAc, 2 mM $Mg(OAc)_2$, $CaCl_2$, 15 % glycerol, 1X protease inhibitor cocktail, 2 mM PMSF, the following TX-100 buffers have the same composition except the indicated concentration of TX-100) and lysed with glass beads. After removal of unbroken cells by two consecutive centrifugations (6500 rpm, 10 min and 10,000 rpm, 20 min), lysates were mixed with the same volume of 2.3% Triton X-100 buffer and rotated at 4 °C for 1 h. The insoluble debris was removed by centrifugation at 14,000 rpm for 30 min. 27.5 μl aliquot was stored for the INPUT fraction. Samples were precleared by incubation with 1.2% Triton X-100 washed protein G-agarose for 1 h at 4 °C and then incubated with washed protein G-agarose and 2 μl of FLAG mouse antibodies overnight. Beads were washed three times with 1.2% Triton X-100 buffer and once with 1% Triton X-100 buffer, and 55 μl of 2X SDS-PAGE sample buffer was added. The INPUT fraction was mixed with 27.5 μl of 2X SDS-PAGE sample buffer. Samples were incubated at 65 °C for 15 min and subjected to SDS-PAGE and western blotting with HA or FLAG rabbit antibodies. The INPUT fractions were treated with Endo H.

Acknowledgments

We thank Mekang Yun for technical assistance and lab members for the critical reading of the manuscript. This research was funded by grants from the National Research Foundation of Korea (NRF-2016R1A2B2013459 and 2019R1A2C2087701) and Promising-Pioneering Research Program through Seoul National University to HK, and the Swiss National Science Foundation (31003A-182519) to MS. SJ is supported by BK21 postdoctoral fellowship program from the National Research Foundation of Korea.

Declaration of Competing Interest

The authors declare that they have no known competing financial interests or personal relationships that could have appeared to influence the work reported in this paper.

Received 20 January 2021;
Accepted 11 June 2021;
Available online 18 June 2021

Keywords:
membrane protein;
Sec61;
Sec62;
topology;
yeast

References

1. Keenan, R.J., Freymann, D.M., Stroud, R.M., Walter, P., (2001). The signal recognition particle. *Annu. Rev. Biochem.*, **70**, 755–775.
2. Wiedmann, M., Huth, A., Rapoport, T.A., (1986). A signal sequence is required for the functions of the signal recognition particle. *Biochem. Biophys. Res. Commun.*, **134**, 790–796.
3. Kurzchalia, T.V. et al, (1986). The signal sequence of nascent preprolactin interacts with the 54K polypeptide of the signal recognition particle. *Nature*, **320**, 634–636.
4. Ast, T., Cohen, G., Schuldiner, M., (2013). A network of cytosolic factors targets SRP-independent proteins to the endoplasmic reticulum. *Cell*, **152**, 1134–1145.
5. Plath, K., Rapoport, T.A., (2000). Spontaneous release of cytosolic proteins from posttranslational substrates before their transport into the endoplasmic reticulum. *J. Cell Biol.*, **151**, 167–178.
6. Chartron, J.W., Hunt, K.C., Frydman, J., (2016). Cotranslational signal-independent SRP preloading during membrane targeting. *Nature*, **536**, 224–228.
7. Jan, C.H., Williams, C.C., Weissman, J.S., (2014). Principles of ER cotranslational translocation revealed by proximity-specific ribosome profiling. *Science*, **346**, 1257521.
8. Costa, E.A., Subramanian, K., Nunnari, J., Weissman, J.S., (2018). Defining the physiological role of SRP in protein-targeting efficiency and specificity. *Science*, **359**, 689–692.
9. Doring, K. et al, (2017). Profiling Ssb-nascent chain interactions reveals principles of Hsp70-assisted folding. *Cell*, **170**, 298–311 e220.
10. Spiess, M., Junne, T., Janoschke, M., (2019). Membrane protein integration and topogenesis at the ER. *Protein J.*,.
11. Li, L. et al, (2016). Crystal structure of a substrate-engaged SecY protein-translocation channel. *Nature*, **531**, 395–399.
12. Shaw, A.S., Rottier, P.J., Rose, J.K., (1988). Evidence for the loop model of signal-sequence insertion into the endoplasmic reticulum. *Proc. Natl. Acad. Sci. USA*, **85**, 7592–7596.

13. Devaraneni, P.K. et al, (2011). Stepwise insertion and inversion of a type II signal anchor sequence in the ribosome-Sec61 translocon complex. *Cell*, **146**, 134–147.
14. Goder, V., Spiess, M., (2003). Molecular mechanism of signal sequence orientation in the endoplasmic reticulum. *EMBO J.*, **22**, 3645–3653.
15. Kocik, L., Junne, T., Spiess, M., (2012). Orientation of internal signal-anchor sequences at the Sec61 translocon. *J. Mol. Biol.*, **424**, 368–378.
16. von Heijne, G., (1986). The distribution of positively charged residues in bacterial inner membrane proteins correlates with the trans-membrane topology. *EMBO J.*, **5**, 3021–3027.
17. Harada, Y., Li, H., Wall, J.S., Li, H., Lennarz, W.J., (2011). Structural studies and the assembly of the heptameric post-translational translocon complex. *J. Biol. Chem.*, **286**, 2956–2965.
18. Deshaies, R.J., Sanders, S.L., Feldheim, D.A., Schekman, R., (1991). Assembly of yeast Sec proteins involved in translocation into the endoplasmic reticulum into a membrane-bound multisubunit complex. *Nature*, **349**, 806–808.
19. Jung, S.J., Kim, J.E., Reithinger, J.H., Kim, H., (2014). The Sec62-Sec63 translocon facilitates translocation of the C-terminus of membrane proteins. *J. Cell Sci.*, **127**, 4270–4278.
20. Reithinger, J.H., Kim, J.E., Kim, H., (2013). Sec62 protein mediates membrane insertion and orientation of moderately hydrophobic signal anchor proteins in the endoplasmic reticulum (ER). *J. Biol. Chem.*, **288**, 18058–18067.
21. Tripathi, A., Mandon, E.C., Gilmore, R., Rapoport, T.A., (2017). Two alternative binding mechanisms connect the protein translocation Sec71-Sec72 complex with heat shock proteins. *J. Biol. Chem.*, **292**, 8007–8018.
22. Wu, X., Cabanos, C., Rapoport, T.A., (2019). Structure of the post-translational protein translocation machinery of the ER membrane. *Nature*, **566**, 136–139.
23. Itskanov, S., Park, E., (2019). Structure of the posttranslational Sec protein-translocation channel complex from yeast. *Science*, **363**, 84–87.
24. Yim, C. et al, (2018). Profiling of signal sequence characteristics and requirement of different translocation components. *Biochim. Biophys. Acta, Mol. Cell. Res.*, **1865**, 1640–1648.
25. Meyer, H.A., Hartmann, E., (1997). The yeast SPC22/23 homolog Spc3p is essential for signal peptidase activity. *J. Biol. Chem.*, **272**, 13159–13164.
26. Nilsson, I.M., von Heijne, G., (1993). Determination of the distance between the oligosaccharyltransferase active site and the endoplasmic reticulum membrane. *J. Biol. Chem.*, **268**, 5798–5801.
27. Goder, V., Junne, T., Spiess, M., (2004). Sec61p contributes to signal sequence orientation according to the positive-inside rule. *Mol. Biol. Cell*, **15**, 1470–1478.
28. Jung, S.J., Jung, Y., Kim, H., (2019). Proper insertion and topogenesis of membrane proteins in the ER depend on Sec63. *Biochim. Biophys. Acta, Gen. Subj.*, **1863**, 1371–1380.
29. Corsi, A.K., Schekman, R., (1997). The lumenal domain of Sec63p stimulates the ATPase activity of BiP and mediates BiP recruitment to the translocon in Saccharomyces cerevisiae. *J. Cell Biol.*, **137**, 1483–1493.
30. Ng, D.T., Brown, J.D., Walter, P., (1996). Signal sequences specify the targeting route to the endoplasmic reticulum membrane. *J. Cell Biol.*, **134**, 269–278.
31. Itskanov, S., Kuo, K.M., Gumbart, J.C., Park, E., (2021). Stepwise gating of the Sec61 protein-conducting channel by Sec63 and Sec62. *Nature Struct. Mol. Biol.*,.
32. Weng, T.H. et al, (2020). Architecture of the active post-translational Sec translocon. *EMBO J.*,, e105643.
33. Young, B.P., Craven, R.A., Reid, P.J., Willer, M., Stirling, C.J., (2001). Sec63p and Kar2p are required for the translocation of SRP-dependent precursors into the yeast endoplasmic reticulum in vivo. *EMBO J.*, **20**, 262–271.
34. Wilkinson, B.M., Tyson, J.R., Stirling, C.J., (2001). Ssh1p determines the translocation and dislocation capacities of the yeast endoplasmic reticulum. *Dev. Cell*, **1**, 401–409.
35. Longtine, M.S. et al, (1998). Additional modules for versatile and economical PCR-based gene deletion and modification in Saccharomyces cerevisiae. *Yeast*, **14**, 953–961.
36. Pilon, M., Schekman, R., Romisch, K., (1997). Sec61p mediates export of a misfolded secretory protein from the endoplasmic reticulum to the cytosol for degradation. *EMBO J.*, **16**, 4540–4548.
37. Zhang, S., Xu, C., Larrimore, K.E., Ng, D.T.W., (2017). Slp1-Emp65: a guardian factor that protects folding polypeptides from promiscuous degradation. *Cell*, **171**, 346–357 e312.